IOP Conf. Series: Journal of Physics: Conf. Series **791** (2017) 012036 doi:10.1088/1742-6596/791/1/012036

Surface states and positron annihilation spectroscopy: results and prospects from a first-principles approach

V Callewaert[1], R Saniz[1], B Barbiellini[2] and B Partoens[1]

[1] Departement Fysica, Universiteit Antwerpen, Groenenborgerlaan 171, B-2020 Antwerpen, Belgium

[2] Department of Physics, Northeastern University, Boston, Massachusetts 02115, USA

E-mail: vincent.callewaert@uantwerpen.be

Abstract. The trapping of positrons at the surface of a material can be exploited to study quite selectively the surface properties of the latter by means of positron annihilation spectroscopy techniques. To support these, it is desirable to be able to theoretically predict the existence of such positronic surface states and to describe their annihilation characteristics with core or valence surface electrons in a reliable way. Here, we build on the well-developed first-principles techniques for the study of positrons in bulk solids as well as on previous models for surfaces, and investigate two schemes that can improve the theoretical description of the interaction of positrons with surfaces. One is based on supplementing the local-density correlation potential with the corrugated image potential at the surface, and the other is based on the weighted-density approximation to correlation. We discuss our results for topological insulators, graphene layers, and quantum dots, with emphasis on the information that can be directly related to experiment. We also discuss some open theoretical problems that should be addressed by future research.

Surface phenomena play a fundamental role in determining the properties of materials of great current interest. Prominent examples are topological insulators and nanostructured systems, such as quantum dots and graphene layers. To study these systems it is preferable to use a technique capable of probing the surface of a material with as little interference from the bulk as possible. Indeed, if the information collected can be ascribed to the response of the surface alone, it can provide deeper and unambiguous insight into the properties of the material studied. Advanced positron annihilation spectroscopy (PAS) techniques are nearly ideally suited for this purpose. Positrons can get trapped at the surface of a material via, e.g., diffusion or Auger Mediated Positron Sticking (AMPS) [1, 2]. In such a case, the radiation following annihilation will contain quite direct information on the surface electronic properties, structure and/or composition [2–4].

To disentangle the information that experiments collect, it would be advantageous to count on theoretical information in various respects. First, it would be useful to know whether a surface can support positronic surface states, and what their binding energies would be. Furthermore, details about annihilation characteristics, such as lifetimes and annihilation probabilities with core and valence electrons, would be of great value. First-principles methods offer the most reliable tools for this purpose. To apply these, however, we face the challenge of describing

properly electron-positron correlations in the surface region. Indeed, while quite reliable approximations to electron-positron correlation for studies in the bulk exist [5], this is not the case for surfaces. The image form of the correlation potential in the vacuum away from the surface is not reproduced by the current approximations, and the appropriate form of electron-positron correlation in the low electron density region at the surface is difficult to model. Although this has been recognised early on [1, 5, 6], a completely satisfactory solution has not been found so far.

The present work is performed in the zero positron density limit of the well-known two-component electron-positron density functional theory [1, 5, 7]. In this limit the positron does not perturb the electron density. We thus calculate the latter following a standard ab initio method. For this we use the VASP ab initio package [8, 9], using the projector-augmented-wave (PAW) method [10] and the Perdew-Burke-Ernzerhof (PBE) functional [11]. We take into account spin-orbit coupling. The density thus obtained is used to calculate the electron-positron correlation potential in the Kohn-Sham hamiltonian for the positron. The Kohn-Sham equations corresponding to the positron are then solved using the Doppler/MIKA package [12].

To model electron-positron correlation at the surface we follow two different approaches, applying them to well-studied systems, as mentioned above. Our first approach consists in using the local-density (LDA) form of the correlation in the bulk region, and supplement it with the corrugated mirror, or image potential, model in the surface region [13]. Specifically, if z is the coordinate perpendicular to the surface, the correlation potential is

$$v_{\rm corr}(\mathbf{r}) = \begin{cases} v_{e\text{-}p}^{\rm LDA}(\mathbf{r}), & z \le z_0 \\ \max(v_{\rm im}(\mathbf{r}), v_{e\text{-}p}^{\rm LDA}(\mathbf{r})), & z > z_0. \end{cases} \tag{1}$$

Here, the corrugated image potential is given by

$$v_{\rm im}(\mathbf{r}) = -\frac{e}{4(z_{\rm eff}(\mathbf{r}) - z_0)}, \tag{2}$$

with z_0 the image potential reference plane and

$$z_{\rm eff}(\mathbf{r}) = \int_{z_0}^{\infty} dz\, z\, \delta(n_e(\mathbf{r}) - \langle n_e \rangle(z)), \tag{3}$$

with n_e the electronic density and the brackets indicating its average over the unit cell in planes parallel to the surface. We applied this model to Bi_2Te_2Se, a well-known topological insulator. A fuller account of our results will be published elsewhere [14]. Here we focus on the existence of a surface state and on some of the information it can yield. We model the system with a four quintuple-layer slab perpendicular to the [111] direction (rhombohedral unit cell), exposing its Te-terminated surface, as in experiment [15]. To give an idea of the potential seen by the positron near the surface, in Fig. 1(a) we plot the average of the potential, over planes parallel to the surface, within the unit cell. One can see that the correlation potential has an incorrect behaviour away from the surface, and deviates sharply from the image potential. The latter is also shown. The total potential shown is the image-potential corrected potential as defined in Eq. (1). The solution of the Kohn-Sham equations results in a positron groundstate residing in the potential well at the surface, with a binding energy $E_b = 2.69$ eV. The experimental binding energy can be deduced as follows. In AMPS measurements, the maximum kinetic energy of the emitted Auger electrons is related to the incident positron energy, E_p, and the positron binding energy by $E_{\rm max} = E_p + E_b - \phi_e$, with ϕ_e the electron work function. Experiment shows that the incident positron threshold energy for Auger electron emission is 1.8 eV [14], i.e., $E_p + E_b - \phi_e = 0$. On the other hand, the positron binding energy is related to the

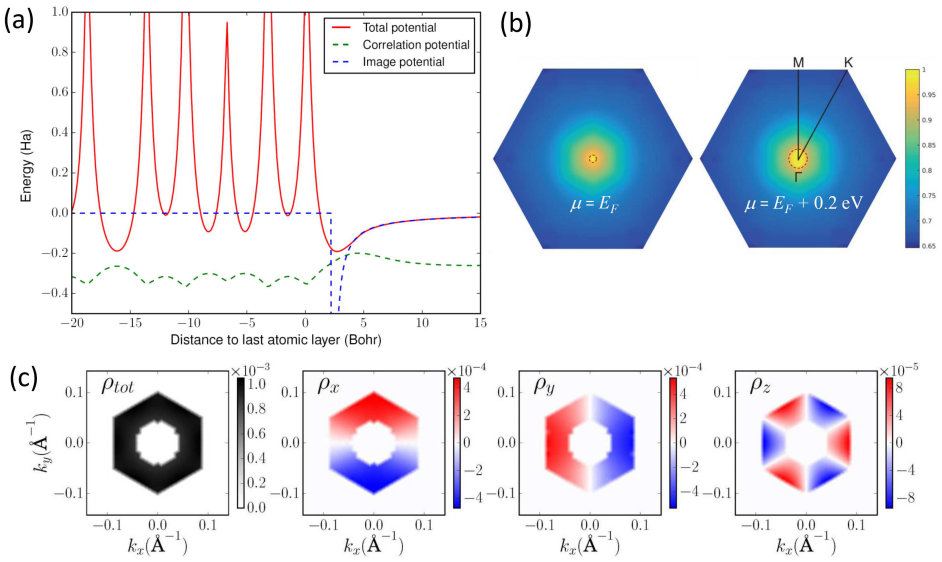

Figure 1. (a) Potential seen by the positron at the surface of Bi_2Te_2Se. The total potential results from replacing the LDA correlation potential away from the surface by the image potential, as in Eq. (1). (b) The LCW maps over the (2D) Brillouin zone of Bi_2Te_2Se, for the electronic chemical potentials indicated in the plots. The break a the Fermi momenta clearly reveals the small circular Fermi surfaces (dotted circles). (c) Magnetisation components for states around the Fermi surface (between E_F and $E_F + 0.2$ eV). The leftmost plot shows the total amplitude of the LCW map. The other plots show the components indicated. (Figs. 1(b) and 1(c) adapted with permission from Ref. 14. Copyrighted by the American Physical Society.)

positronium thermal activation energy, E_a, by $E_b = E_a - \phi_e + 6.8$ eV [16]. Given that E_a has been measured to be 0.4 eV [14,17], the experimental value of E_b is found to be 2.7 eV, showing excellent agreement between theory and experiment. We consider now the possible information that the annihilation of such a state can deliver. In Bi_2Te_2Se, the Fermi level is just above the Dirac point (and can actually be tuned by alloying with Sb), so the Fermi surface consists of a relatively small circle around the Γ point [15]. Since the positron is at the surface and the Dirac cone in Bi_2Te_2Se arises from electronic surface states, two-dimensional angular correlation of annihilation radiation (2D-ACAR) measurements can be expected to detect the Fermi surface. In Fig. 1(b) we show the calculated Lock-Crisp-West (LCW) maps [18] for two different values of the electronic chemical potential, namely at the undoped material Fermi energy value, and 0.2 eV above it. The Fermi surface is indicated by the dotted line. We note that the drop in intensity at the Fermi momenta is 5%-7%, so should be clearly observable in experiment. Indeed, the drop is much larger than the 1% in the case of the $Nd_{2-x}Ce_xCuO_{4-\delta}$, in which 2D-ACAR has been successfully applied to map the Fermi surface [19] and, moreover, the momentum resoltion of current 2D-ACAR spectrometers is sufficiently high [20]. A further feature of the Dirac cone that is important, but difficult to observe experimentally, is the spin texture associated with the hexagonal warping [21,22]. We can extract the signal from the Dirac cone in the vicinity of the Fermi surface by taking the difference of the LCW maps at $\mu = E_F + 0.2$ eV and $\mu = E_F$. The magnetisation components of the momentum density from the Dirac cone should be observable using spin-polarised positron beams. The calculated magnetisation components in the region delimited by the two chemical potentials mentioned are shown in Fig. 1(c). These clearly show (i) the hexagonal warping as momenta move away from the Fermi surface, (ii) that the in-plane (xOy) magnetisation rotates (clockwise) with momentum, and (iii) that there is an out-of-plane

(z direction) component that increases with warping. Thus, these important features can be experimentally studied using spin-polarised PAS techniques.

As mentioned in the introduction, quantum dots and nanocrystals are among the systems in which surface states are determinant. PAS techniques, such as 2D-ACAR and positron annihilation lifetime spectroscopy (PALS) were used to show that positrons can get trapped at the surface of CdSe and PbSe nanocrystals [3, 4]. We applied the preceding scheme to see if we could observe these states and calculate their binding energy. We modeled the surface of the nanocrystals with slabs. Our first results indicated that while for CdSe the potential well at the surface was deep enough to trap a positron, this was not the case in PbSe. Also, in the case of CdSe, the positron state seems to overlap more strongly with the surface than in experiment, resulting in a too short lifetime. At this point we must recognize that the approach based on Eq. (1) is ad hoc, and there is no guarantee that it is reliable in all cases. Our second approach to describing a positron at the surface of a solid is based on the the weighted-density approximation (WDA) [23], as modified by Rubaszek for positron surface states [24, 25]. It relies on a non-local electron-positron correlation functional that connects smoothly the LDA correlation inside the solid to the mirror-like correlation far outside from the surface. Rubaszek used it to describe positron states at the surface of metals, describing the latter with the jellium model. Briefly, the electron-positron correlation potential can be written

$$v_{e\text{-}p}(\mathbf{r}_p) = -\frac{1}{2}\int d\mathbf{r}_e \frac{\Delta n_c(\mathbf{r}_e|\mathbf{r}_p)}{|\mathbf{r}_e - \mathbf{r}_p|}, \tag{4}$$

with the screening cloud given by $\Delta n_c(\mathbf{r}_e|\mathbf{r}_p) = n_e(\mathbf{r}_e)[g_{n_e}(\mathbf{r}_e|\mathbf{r}_p) - 1]$, where g_{n_e} is the electron positron pair correlation function (a functional of the electron density and dependent on the electron and positron coordinates) [26]. In the LDA approximation,

$$\Delta n_c^{\mathrm{LDA}}(\mathbf{r}_e|\mathbf{r}_p) = n_e(\mathbf{r}_p)[g_{n_e(\mathbf{r}_p)}(|\mathbf{r}_p - \mathbf{r}_e|) - 1], \tag{5}$$

i.e., the pair correlation function is given the form it has for a positron in a homogeneous electron gas (n_e is evaluated at the position of the positron only and the pair correlation function depends on the distance between electron and positron). In the WDA, the screening cloud is written

$$\Delta n_c^{\mathrm{WDA}}(\mathbf{r}_e|\mathbf{r}_p) = n_e(\mathbf{r}_e)[g_{n^*(\mathbf{r}_p)}(|\mathbf{r}_p - \mathbf{r}_e|) - 1]. \tag{6}$$

Here, the n_e is evaluated at the position $\mathbf{r}_e$. In contrast with the LDA, the screening cloud depends non-locally on the electron density. The pair correlation has the same form as in the LDA, but it depends on an effective, or "weighted" density, obeying to the sum rule

$$\int d\mathbf{r}_e \Delta n_c^{\mathrm{WDA}}(\mathbf{r}_e|\mathbf{r}_p) = 1. \tag{7}$$

We first applied this approach to our Bi_2Te_2Se, and CdSe and PbSe surfaces. In the first case, the WDA and the LDA+corrugated image potential surface states are nearly the same. Our preliminary results in the case of CdSe and PbSe, on the other hand, show a stronger difference. In particular, the positron state in PbSe is clearly located on the vacuum side of the slab, instead of between the first and second layer of the material (which is the case in the LDA+corrugated image potential approach). In the case of CdSe, the positron surface state is similarly pushed further away from the surface. We note, however, that these systems are more complicated than layered systems like Bi_2Te_2Se in that surface relaxation is stronger and therefore more difficult to describe accurately and compare with experiment. In the case of Bi_2Te_2Se, experiments are carried out on nearly perfect surfaces, so comparison with calculations is more straightforward. In the case of the nanocrystals, it might be necessary to take into account the effect of the

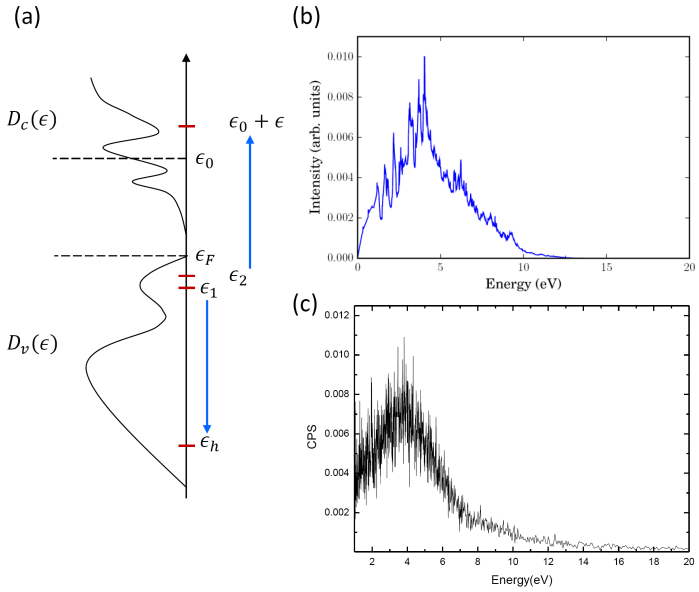

Figure 2. (a) Illustration of a VVV PAES process. A positron creates a hole in the valence band at energy ϵ_h. An electron with energy ϵ_1 recombines with the hole, transferring the energy difference to an electron of energy ϵ_2 that might escape if its final energy is above the vacuum level, ϵ_0. Plots (b) and (c) show the calculated and measured Auger spectra, respectively, showing remarkable overall agreement.

ligands [3,4] in our calculations. Further research is necessary to verify our results and to obtain lifetimes and other annihilation characteristics.

We further applied this approach to determine whether a nanofilm of graphene sustains a positron surface state and, if so, to calculate its wavefunction. This is another layered system of great interest because recent experiments by Weiss and co-workers strongly suggest that in their positron-annihilation Auger-electron spectroscopy (PAES) measurements they have observed VVV processes, i.e., Auger processes involving solely valence states (in contrast to standard Auger spectroscopy, where the initial hole is at a core state) [27]. The process is illustrated in Fig. 2(a). Given the positron surface state wavefunction, the rate at which it annihilates with a valence electron with energy ϵ_h (thus creating an initial hole there) is readily given by

$$\lambda(\epsilon_h) = \frac{1}{\Omega_{\mathrm{BZ}}} \sum_i \int_{\Omega_{\mathrm{BZ}}} d\mathbf{k} \lambda_i(\mathbf{k}) f(\epsilon_i(\mathbf{k}))\, \delta(\epsilon_h - \epsilon_i(\mathbf{k})), \tag{8}$$

with f the Fermi distribution and the annihilation rate with an electron in band i and momentum $\mathbf{k}$ given as usual by $\lambda_i(\mathbf{k}) = \pi r_e^2 c \int d\mathbf{r} |\psi_{i,\mathbf{k}}(\mathbf{r})|^2 |\psi_p(\mathbf{r})|^2 \gamma(n_e(\mathbf{r}))$, where ψ_p denotes the positron wavefunction and γ the enhancement factor [1, 5]. Following the work of Hagstrum on Auger processes [28], the Auger spectrum in our case is given by

$$A(\epsilon) = \int d\epsilon_h\, d\epsilon_1\, d\epsilon_2 \lambda(\epsilon_h) D_v(\epsilon_1) \Theta(\epsilon_1 - \epsilon_h) D_v(\epsilon_2) D_c(\epsilon_0 + \epsilon) P(\epsilon_2, \epsilon) \delta((\epsilon_1 - \epsilon_h) + (\epsilon_2 - \epsilon_0 - \epsilon)). \tag{9}$$

Here D_v and D_c denotes the valence and conduction bands densities of states, ϵ_0 is the vacuum level energy, and $P(\epsilon_2, \epsilon) = [1 - \sqrt{(\epsilon_0 - \epsilon_2)/(\epsilon_0 + \epsilon - \epsilon_2)}]/2$ is the electron "escape function" [28]. The calculations were done for a graphene layer. Fig. 2(b) shows the calculated Auger spectrum, while Fig. 2(c) shows one of various preliminary experimental results. The common feature in

experiment is a dominant peak around 4 eV, in striking coincidence with experiment. Further details will be presented in a forthcoming publication. The main purpose here is to show the usefulness of first-principles calculations and the power of PAS techniques.

Acknowledgments
We thank A. Weiss for very useful conversations and for his preliminary Auger results. We further benefited from clarifying discussions with S. Eijt on the positron annihilation characteristics of the nanocrystals investigated in his laboratory. We acknowledge financial support from FWO-Vlaanderen (projects G.0150.13 and G.0224.14N). This work was carried out using the HPC infrastructure of the University of Antwerp (CalcUA), a division of the Flemish Supercomputer Center (VSC), funded by the Hercules foundation and the Flemish Government (EWI Department). The work at Northeastern University was supported by the US Department of Energy (DOE), Office of Science, Basic Energy Sciences grant number DE-FG02-07ER46352 (core research), and benefited from Northeastern University's Advanced Scientific Computation Center (ASCC), the NERSC supercomputing center through DOE grant number DE-AC02-05CH11231, and support (applications to layered materials) from the DOE EFRC: Center for the Computational Design of Functional Layered Materials (CCDM) under DE-SC0012575.

References
[1] Puska M J and Nieminen R M 1994 *Rev. Mod. Phys.* **66** 841
[2] Mukherjee S, Nadesalingam M P, Guagliardo P, Sergeant A D, Barbiellini B, Williams J F, Fazleev N G and Weiss A H 2010 *Phys. Rev. Lett.* **104** 247403
[3] Eijt S W H, Van Veen A, Schut H, Mijnarends P E, Denison A B, Barbiellini B and Bansil A 2006 *Nat. Mater.* **5** 23
[4] Chai L *et al.* 2013 *APL Materials* **1** 022111
[5] Tuomisto F and Makkonen I 2013 *Rev. Mod. Phys.* **85** 1583
[6] Rubaszek A, Kiejna A and Daniuk S 1993 *J. Phys.: Condens. Matter* **5** 8195
[7] The zero density limit of the two-component density-fnctional theory remains valid at a perfect surface as the positron ground state will be delocalized in at least in the two directions parallel to the surface.
[8] Kresse G and Furthmüller J 1996 *Comput. Mat. Sci.* **6** 15
[9] Kresse G and Furthmüller 1996 *Phys. Rev. B* **54** 11169
[10] Kresse G and Joubert D 1999 *Phys. Rev. B* **59** 1758
[11] Perdew J P, Burke K and Ernzerhof M 1996 *Phys. Rev. Lett.* **77** 3865
[12] Makkonen I, Hakala M and Puska M J 2006 *Phys. Rev. B* **73** 035103
[13] Nieminen R M and Puska M J 1983 *Phys. Rev. Lett.* **50** 281
[14] Callewaert V, Shastry K, Saniz R, Makkonen I, Barbiellini B, Assaf B A, Heiman D, Moodera J S, Partoens B, Bansil A and Weiss A H 2016 *Phys. Rev. B* **94** 115411
[15] Neupane M *et al.* 2012 *Phys. Rev. B* **85** 235406
[16] Chu S, Mills A P and Murray C A 1981 *Phys. Rev. B* **23** 2060
[17] Shastry K, Weiss A H, Barbiellini B, Assaf B A, Lim Z H, Joglekar P V and Heiman D 2015 *J. Phys. Conf. Ser.* **618** 012006
[18] Lock D G, Crisp V H C and West R N 1973 *J. Phys. F: Metal Phys.* **3** 561
[19] Shukla A, Barbiellini B, Hoffmann L, Manuel A A, Sadowski W S, Walker E and Peter M 1996 *Phys. Rev. B* **53** 3613
[20] Dugdale S B, Laverock J, Utfeld C, Alam M A, Haynes T D, Billington D and Ernsting D 2013 *J. Phys. Conf. Ser.* **443** 012083
[21] Basak S, Lin H, Wray L A, Xu S Y, Hasan M Z and Bansil A 2011 *Phys. Rev. B* **84** 121401
[22] Fu L 2009 *Phys. Rev. Lett.* **103** 266801
[23] Gunnarsson O, Jonson M and Lundqvist B I 1979 *Phys. Rev. B* **20** 3136
[24] Rubaszek A 1989 *J. Phys.: Condens. Matter* **1** 2141
[25] Rubaszek A 1991 *Phys. Rev. B* **44** 10857
[26] Note that it can be shown that if the generalised-gradient approximation (Barbiellini B and Kuriplach J 2015 *Phys. Rev. Lett.* **114** 147401) were used instead of the LDA, the correlation potential outside the surface would have an unphysical faster-than-exponential decay.
[27] Chirayath V A *et al* 2016 arXiv:1610.09575v2 [cond-mat.mess-hall]
[28] Hagstrum H D 1954 *Phys. Rev.* **96** 336; 1961 *Phys. Rev.* **122** 83